

World Journal of *Clinical Cases*

World J Clin Cases 2020 August 6; 8(15): 3136-3376



OPINION REVIEW

- 3136 Impacts and challenges of United States medical students during the COVID-19 pandemic
Rolak S, Keefe AM, Davidson EL, Aryal P, Parajuli S
- 3142 Recent advances in the management of gastrointestinal stromal tumor
Ahmed M
- 3156 Medical research during the COVID-19 pandemic
AlNaamani K, AlSinani S, Barkun AN

REVIEW

- 3164 Progress of intravoxel incoherent motion diffusion-weighted imaging in liver diseases
Tao YY, Zhou Y, Wang R, Gong XQ, Zheng J, Yang C, Yang L, Zhang XM

MINIREVIEWS

- 3177 Typical and atypical COVID-19 computed tomography findings
Caruso D, Polidori T, Guido G, Nicolai M, Bracci B, Cremona A, Zerunian M, Polici M, Pucciarelli F, Rucci C, Dominici CD, Girolamo MD, Argento G, Sergi D, Laghi A
- 3188 Review of possible psychological impacts of COVID-19 on frontline medical staff and reduction strategies
Fu XW, Wu LN, Shan L

CLINICAL AND TRANSLATIONAL RESEARCH

- 3197 Overexpression of AMPD2 indicates poor prognosis in colorectal cancer patients *via* the Notch3 signaling pathway
Gao QZ, Qin Y, Wang WJ, Fei BJ, Han WF, Jin JQ, Gao X

ORIGINAL ARTICLE**Case Control Study**

- 3209 Effect of motivational interviewing on postoperative weight control in patients with obstructive sleep apnea-hypopnea syndrome
Sun XH, Xue PS, Qi XX, Fan L

Retrospective Study

- 3218 Thalidomide for refractory gastrointestinal bleeding from vascular malformations in patients with significant comorbidities
Bayudan AM, Chen CH

- 3230** Colorectal adenocarcinoma patients with M1a diseases gain more clinical benefits from palliative primary tumor resection than those with M1b diseases: A propensity score matching analysis

Li CL, Tang DR, Ji J, Zang B, Chen C, Zhao JQ

- 3240** Surgical outcomes of bladder augmentation: A comparison of three different augmentation procedures

Sun XG, Wang RY, Xu JL, Li DG, Chen WX, Li JL, Wang J, Li AW

Clinical Trials Study

- 3249** Comparison of measurements of anterior chamber angle *via* anterior segment optical coherence tomography and ultrasound biomicroscopy

Yu ZY, Huang T, Lu L, Qu B

Observational Study

- 3259** Dydrogesterone treatment for menstrual-cycle regularization in abnormal uterine bleeding – ovulation dysfunction patients

Wang L, Guan HY, Xia HX, Chen XY, Zhang W

CASE REPORT

- 3267** Multi-organ IgG4-related disease continues to mislead clinicians: A case report and literature review

Strainiene S, Sarlauskas L, Savlan I, Liakina V, Stundiene I, Valantinas J

- 3280** *Campylobacter jejuni* enterocolitis presenting with testicular pain: A case report

Sanagawa M, Kenzaka T, Kato S, Yamaoka I, Fujimoto S

- 3284** Natural killer/T-cell lymphoma with intracranial infiltration and Epstein-Barr virus infection: A case report

Li N, Wang YZ, Zhang Y, Zhang WL, Zhou Y, Huang DS

- 3291** Successful management of tubular colonic duplication using a laparoscopic approach: A case report and review of the literature

Li GB, Han JG, Wang ZJ, Zhai ZW, Tao Y

- 3299** Hypothyroidism with elevated pancreatic amylase and lipase without clinical symptoms: A case report

Xu YW, Li R, Xu SC

- 3305** Two mechanically ventilated cases of COVID-19 successfully managed with a sequential ventilation weaning protocol: Two case reports

Peng M, Ren D, Liu YF, Meng X, Wu M, Chen RL, Yu BJ, Tao LC, Chen L, Lai ZQ

- 3314** Adult duodenal intussusception with horizontal adenoma: A rare case report

Wang KP, Jiang H, Kong C, Wang LZ, Wang GY, Mo JG, Jin C

- 3320** Isolated metachronous splenic multiple metastases after colon cancer surgery: A case report and literature review

Hu L, Zhu JY, Fang L, Yu XC, Yan ZL

- 3329** Imaging of hemorrhagic primary central nervous system lymphoma: A case report
Wu YW, Zheng J, Liu LL, Cai JH, Yuan H, Ye J
- 3334** Coexistence of ovarian serous papillary cystadenofibroma and type A insulin resistance syndrome in a 14-year-old girl: A case report
Yan FF, Huang BK, Chen YL, Zhuang YZ, You XY, Liu CQ, Li XJ
- 3341** Acute suppurative oesophagitis with fever and cough: A case report
Men CJ, Singh SK, Zhang GL, Wang Y, Liu CW
- 3349** Computed tomography, magnetic resonance imaging, and F-deoxyglucose positron emission computed tomography/computed tomography findings of alveolar soft part sarcoma with calcification in the thigh: A case report
Wu ZJ, Bian TT, Zhan XH, Dong C, Wang YL, Xu WJ
- 3355** COVID-19 with asthma: A case report
Liu AL, Xu N, Li AJ
- 3365** Total laparoscopic segmental gastrectomy for gastrointestinal stromal tumors: A case report
Ren YX, He M, Ye PC, Wei SJ
- 3372** Facial and bilateral lower extremity edema due to drug-drug interactions in a patient with hepatitis C virus infection and benign prostate hypertrophy: A case report
Li YP, Yang Y, Wang MQ, Zhang X, Wang WJ, Li M, Wu FP, Dang SS

ABOUT COVER

Editorial Board Member of *World Journal of Clinical Cases*, Dr. Romano is Professor of Medicine-Gastroenterology at the University of Campania “Luigi Vanvitelli” in Naples, Italy. Dr. Romano received his MD degree cum Laude at the University Federico II in Naples, Italy in 1980 and, after 4 year of Post-Graduate course, he became Specialist in Gastroenterology and Gastrointestinal Endoscopy. Dr. Romano’s research interest was on the cross-talk between H. pylori and gastric epithelial cells, and presently is mainly focused on H. pylori eradication therapy and on the role of nutraceuticals in gastrointestinal diseases. Dr. Romano is presently the Chief of the Endoscopy and Chronic Inflammatory Gastrointestinal Disorders Unit, and Teacher at the University of Campania “Luigi Vanvitelli” in Naples, Italy.

AIMS AND SCOPE

The primary aim of *World Journal of Clinical Cases (WJCC, World J Clin Cases)* is to provide scholars and readers from various fields of clinical medicine with a platform to publish high-quality clinical research articles and communicate their research findings online.

WJCC mainly publishes articles reporting research results and findings obtained in the field of clinical medicine and covering a wide range of topics, including case control studies, retrospective cohort studies, retrospective studies, clinical trials studies, observational studies, prospective studies, randomized controlled trials, randomized clinical trials, systematic reviews, meta-analysis, and case reports.

INDEXING/ABSTRACTING

The *WJCC* is now indexed in Science Citation Index Expanded (also known as SciSearch®), Journal Citation Reports/Science Edition, PubMed, and PubMed Central. The 2020 Edition of Journal Citation Reports® cites the 2019 impact factor (IF) for *WJCC* as 1.013; IF without journal self cites: 0.991; Ranking: 120 among 165 journals in medicine, general and internal; and Quartile category: Q3.

RESPONSIBLE EDITORS FOR THIS ISSUE

Electronic Editor: Yan-Xia Xing, Production Department Director: Yun-Xiaojuan Wu, Editorial Office Director: Jin-Lei Wang.

NAME OF JOURNAL

World Journal of Clinical Cases

ISSN

ISSN 2307-8960 (online)

LAUNCH DATE

April 16, 2013

FREQUENCY

Semimonthly

EDITORS-IN-CHIEF

Dennis A Bloomfield, Sandro Vento, Bao-Gan Peng

EDITORIAL BOARD MEMBERS

<https://www.wjgnet.com/2307-8960/editorialboard.htm>

PUBLICATION DATE

August 6, 2020

COPYRIGHT

© 2020 Baishideng Publishing Group Inc

INSTRUCTIONS TO AUTHORS

<https://www.wjgnet.com/bpg/gerinfo/204>

GUIDELINES FOR ETHICS DOCUMENTS

<https://www.wjgnet.com/bpg/GerInfo/287>

GUIDELINES FOR NON-NATIVE SPEAKERS OF ENGLISH

<https://www.wjgnet.com/bpg/gerinfo/240>

PUBLICATION ETHICS

<https://www.wjgnet.com/bpg/GerInfo/288>

PUBLICATION MISCONDUCT

<https://www.wjgnet.com/bpg/gerinfo/208>

ARTICLE PROCESSING CHARGE

<https://www.wjgnet.com/bpg/gerinfo/242>

STEPS FOR SUBMITTING MANUSCRIPTS

<https://www.wjgnet.com/bpg/GerInfo/239>

ONLINE SUBMISSION

<https://www.f6publishing.com>

Progress of intravoxel incoherent motion diffusion-weighted imaging in liver diseases

Yun-Yun Tao, Yi Zhou, Ran Wang, Xue-Qin Gong, Jing Zheng, Cui Yang, Lin Yang, Xiao-Ming Zhang

ORCID number: Yun-Yun Tao 0000-0001-5081-331; Yi Zhou 0000-0002-1911-5380; Ran Wang 0000-0002-7013-4923; Xue-Qin Gong 0000-0001-8389-8765; Jing Zheng 0000-0002-2031-0845; Cui Yang 0000-0001-6751-9075; Lin Yang 0000-0001-8746-9255; Xiao-Ming Zhang 0000-0001-5327-8506.

Author contributions: Tao YY and Zhou Y are co-first authors; Tao YY and Zhou Y wrote the paper; Yang L revised the paper; Zhang XM designed the research; Wang R, Gong XQ, Zheng J and Yang C collected the data.

Supported by the Projects of the Department of Science and Technology of Sichuan Province, No. 2016JY0105.

Conflict-of-interest statement: The authors declare no conflict of interest with respect to this article.

Open-Access: This article is an open-access article that was selected by an in-house editor and fully peer-reviewed by external reviewers. It is distributed in accordance with the Creative Commons Attribution NonCommercial (CC BY-NC 4.0) license, which permits others to distribute, remix, adapt, build upon this work non-commercially, and license their derivative works on different terms, provided the

Yun-Yun Tao, Yi Zhou, Ran Wang, Xue-Qin Gong, Jing Zheng, Cui Yang, Lin Yang, Xiao-Ming Zhang, Sichuan Key Laboratory of Medical Imaging, Department of Radiology and Medical Research Center of Affiliated Hospital of North Sichuan Medical College, Nanchong 637000, Sichuan Province, China

Corresponding author: Lin Yang, MD, Chief Doctor, Professor, Sichuan Key Laboratory of Medical Imaging, Department of Radiology and Medical Research Center of Affiliated Hospital of North Sichuan Medical College, No. 63 Wenhua Road, Nanchong 637000, Sichuan Province, China. linyangmd@163.com

Abstract

Traditional magnetic resonance (MR) diffusion-weighted imaging (DWI) uses a single exponential model to obtain the apparent diffusion coefficient to quantitatively reflect the diffusion motion of water molecules in living tissues, but it is affected by blood perfusion. Intravoxel incoherent motion (IVIM)-DWI utilizes a double-exponential model to obtain information on pure water molecule diffusion and microcirculatory perfusion-related diffusion, which compensates for the insufficiency of traditional DWI. In recent years, research on the application of IVIM-DWI in the diagnosis and treatment of hepatic diseases has gradually increased and has achieved considerable progress. This study mainly reviews the basic principles of IVIM-DWI and related research progress in the diagnosis and treatment of hepatic diseases.

Key words: Magnetic resonance imaging; Diffusion magnetic resonance imaging; Liver diseases; Liver cirrhosis; Carcinoma; Cholangiocarcinoma

©The Author(s) 2020. Published by Baishideng Publishing Group Inc. All rights reserved.

Core tip: Intravoxel incoherent motion diffusion-weighted imaging (IVIM-DWI) utilizes a double-exponential model to obtain information on pure water molecule diffusion and microcirculatory perfusion-related diffusion, which makes up for the insufficiency of traditional DWI. In recent years, research on the application of IVIM-DWI in the diagnosis and treatment of hepatic diseases has gradually increased and has made great progress. This study mainly reviews the basic principles of IVIM-DWI and its research progress in the diagnosis and treatment of hepatic diseases.

original work is properly cited and the use is non-commercial. See: <http://creativecommons.org/licenses/by-nc/4.0/>

Manuscript source: Unsolicited manuscript

Received: March 26, 2020

Peer-review started: March 26, 2020

First decision: May 29, 2020

Revised: June 11, 2020

Accepted: July 14, 2020

Article in press: July 14, 2020

Published online: August 6, 2020

P-Reviewer: Fiore M, Zhou M

S-Editor: Gong ZM

L-Editor: Webster JR

E-Editor: Liu JH



Citation: Tao YY, Zhou Y, Wang R, Gong XQ, Zheng J, Yang C, Yang L, Zhang XM. Progress of intravoxel incoherent motion diffusion-weighted imaging in liver diseases. *World J Clin Cases* 2020; 8(15): 3164-3176

URL: <https://www.wjgnet.com/2307-8960/full/v8/i15/3164.htm>

DOI: <https://dx.doi.org/10.12998/wjcc.v8.i15.3164>

INTRODUCTION

Magnetic resonance diffusion-weighted imaging (MR-DWI) uses a single exponential model to obtain the apparent diffusion coefficient (ADC) to quantitatively reflect the diffusion motion of water molecules in tissues^[1]. However, voxels also contain diffusion information other than the diffusion motion of pure water molecules, namely, the microcirculatory perfusion of the capillary network in tissues^[1-4]. The ADC values obtained by traditional DWI contain two types of information: Water molecule diffusion and microcirculatory perfusion. The intravoxel incoherent motion (IVIM)-DWI theory was initially proposed by Le Bihan *et al*^[4,5] in the 1980s; IVIM-DWI can obtain quantitative information on pure water molecule diffusion and microcirculatory perfusion-related diffusion and thus compensate for the shortcomings of traditional DWI. This modality can also more accurately and truly reflect the characteristics of tissue structure and pathological changes. Since 1999, when Yamada *et al*^[6] for the first time applied IVIM-DWI technology to the liver, the research on liver IVIM-DWI has gradually increased and has made great progress. This study reviews the basic principles of IVIM-DWI and related research progress in the diagnosis and treatment of hepatic diseases.

BASIC PRINCIPLES OF IVIM-DWI

IVIM-DWI originated from diffusion-weighted magnetic resonance imaging (MRI). MR-DWI can noninvasively detect the diffusion motion of water molecules (water molecules in fluid exhibit microscopic erratic random movement, known as Brownian motion), which reflects the biological characteristics of the tissue. When the signal derives from biological tissues, some factors attenuate the diffusion motion according to different diffusion coefficients, representing the ADC, which is the sum of the contributions of all motion-related diffusion coefficients. The MR signal can be expressed by a single exponential equation:

$$S_b/S_0 = \exp(-b \times ADC).$$

Where b is the diffusion-sensitive gradient with a unit of s/mm^2 ; S_b represents the signal obtained at a particular b value; and S_0 represents a signal that does not apply a diffusion gradient^[7].

IVIM-DWI uses multiple b values and a double-exponential model for image acquisition and analysis, and simultaneously obtains information regarding pure water molecular diffusion and microcirculatory perfusion-related diffusion. IVIM-DWI measures perfusion based on the following assumption: The effects of incoherent motion and blood movement can be separated from other incoherent effects. The IVIM-DWI model assumes that other sources of incoherent signals (water exchange between blood and tissue) are negligible compared with blood flow. In the IVIM-DWI model, the relationship between the degree of local signal attenuation in the tissue and the b value can be expressed by the following formula^[8]:

$$S_b/S_0 = (1-f) \times \exp(-b \times D) + f \times \exp(-b \times D^*).$$

Where D is the simple diffusion coefficient, also known as slow the apparent diffusion coefficient (D_{slow}), which reflects the diffusion motion of pure water molecules in the tissue of interest; D^* is the pseudo-diffusion coefficient, also known as the fast apparent diffusion coefficient (D_{fast}), which reflects the microcirculatory perfusion in the capillary network in the area of interest; and f is the fraction of the fast apparent diffusion coefficient, which represents the volume ratio of the correlation effect of the local microcirculatory perfusion to the total diffusion effect and can be used to determine the blood volume in the area of interest. According to the formula, since D^* is obviously higher than D , the information obtained from a low b value ($< 200 s/mm^2$) mainly reflects the microcirculatory perfusion effect, while the signal attenuation obtained by a high b value ($\geq 200 s/mm^2$) mainly reflects the diffusion effect^[5,9]. Some researchers^[10] believe that $f \times D^*$ should be used as a new cyclic

parameter and that its potential pathophysiological effects should be further elaborated in future studies.

Multiple b values are required for IVIM-DWI to separate tissue diffusion information from perfusion information. Theoretically, more b values correspond to a more accurate data fit and thus better image quality. However, a longer data collection time corresponds to more clinical application limitations. The number of b values used in published studies ranges from 4 to 16, with many studies using approximately 10 b values^[6,9,11,12]. In terms of the distribution of b values, Cohen *et al.*^[13] studied the influence of low b values on D^* and showed that at least two b values below 50 s/mm² are required to ensure that D^* is not underestimated. Koh *et al.*^[14] proposed selecting fewer high b values and more low b values to focus data collection on the sensitive range of perfusion. At present, no consensus on the choice of b values is available, and optimization research on the number and distribution of b values is ongoing^[11,15-17]. For clinical research, the choice of b values should be based on the different tissues tested and the purpose of the evaluation. The factors influencing the measurement results of IVIM-DWI are complex. In addition to b values, scanner and field intensities^[11], the diffusion gradient and respiratory mode^[18,19], the DWI sequence^[20,21], other physiological activities (such as glandular secretions and fluid flow in glandular canals)^[22], motion artefacts, fitting technology and region of interest (ROI) settings^[23-28] can all affect the IVIM-DWI image quality and repeatability of the data. These should also be considered in the clinical study design.

NONALCOHOLIC FATTY LIVER DISEASE

In recent years, the prevalence of fatty liver disease in China has gradually increased, and the onset of the disease is trending to involve younger patients. Approximately 20% of noninvasive nonalcoholic fatty liver disease (NAFLD) cases develop into nonalcoholic steatohepatitis, which can progress to hepatic fibrosis or even cirrhosis^[29]. Studies have shown that^[30-33] the histological characteristics of nonalcoholic hepatic steatosis significantly affect the IVIM-DWI parameters. Parente *et al.*^[31] used IVIM-DWI to study type II diabetic patients with or without NAFLD and found that both the D value and D^* value of fatty livers were significantly lower than those of non-fatty livers. The decrease in the D^* value reflects the decrease in hepatic perfusion caused by hepatic steatosis, whereas the decrease in the D value may be caused by hepatocytomegaly, the deposition of intracellular fat and the simultaneous restriction of water molecule diffusion intracellularly and extracellularly^[33]. The study by Joo *et al.*^[34] showed that the f value of NAFLD livers was significantly lower than that of normal livers, and this f value is associated with the severity of NAFLD.

HEPATIC FIBROSIS

Although percutaneous liver biopsy can determine the severity of hepatic fibrosis, this test is invasive, and its clinical application is limited. IVIM-DWI has important value in the evaluation of hepatic fibrosis^[9,12,19,35-47].

Studies^[12,44,45] have shown that the D , D^* and f values of hepatic fibrosis patients were significantly lower than those in normal control groups. The IVIM-DWI parameters D , D^* and f can be used to distinguish healthy people from patients with hepatic fibrosis, with the f value exhibiting the best diagnostic value^[38]. The study by Shiraga *et al.*^[36] showed that IVIM-DWI also identified a pre-fibrotic state of the liver in Fontan patients. The study included five consecutive Fontan patients and four age-matched healthy volunteers. The results showed that in the five Fontan patients, laboratory tests and ultrasound showed almost normal liver conditions, and cardiac catheterization and MRI showed good Fontan circulation, but the D , D^* and f values of Fontan patients were significantly lower than those of the control group. However, some studies^[9,41,46] have shown that the D value was not significantly different between normal liver tissue and hepatic fibrosis tissue. Dyvorne *et al.*^[19] showed that D^* values were not significantly different between normal volunteers and patients with hepatic fibrosis.

In addition, many studies have focused on the use of IVIM-DWI technology to determine the severity of hepatic fibrosis, but the conclusions are not completely consistent^[12,37-45,47]. Hu *et al.*^[40,45] showed that IVIM-DWI-related parameters were negatively correlated with hepatic fibrosis stages, with the D , D^* and f value decreasing with increases in the severity of hepatic fibrosis. Chen *et al.*^[45] used IVIM-

DWI to scan 25 patients with hepatic fibrosis and 25 healthy volunteers. The results showed that the ADC, D, D* and f values in the hepatic cirrhosis group were significantly lower than those in the control group. Additionally, significant differences were found in the parameters of hepatic fibrosis stages (the F0-1 group and F2-4 group and the F0-2 group and F3-4 group). However, further studies have shown that some parameters are not correlated with the hepatic fibrosis stage^[37-39,41-44]. For example, Chung *et al.*^[41-44] showed that a higher stage of hepatic fibrosis corresponded to lower D* and f values; however, no correlation was found between the D values and the stages of hepatic fibrosis. On the other hand, Hu *et al.*^[39] observed a difference only in the D* values in different fibrosis groups. Other studies^[48-51] have shown that IVIM-DWI is not sufficient for staging hepatic fibrosis (Table 1). The different D and D* values in the same disease of the previous studies maybe due to the following reasons: (1) The number of patients with each stage of disease was different; (2) The number of b values or an uneven b value distribution may limit the fitting precision; (3) D* has high uncertainty and poor reproducibility; and (4) D values were influenced by steatosis and iron overload^[19,45,50].

In summary, the IVIM-DWI parameters of hepatic fibrosis tissues show a decreasing trend compared with those of normal hepatic tissues, and IVIM-DWI can be used for the diagnosis of hepatic fibrosis; however, the value of applying IVIM-DWI for hepatic fibrosis staging still requires further exploration.

DIFFERENTIATION OF BENIGN AND MALIGNANT HEPATIC TUMORS

A large number of studies have discussed the application of IVIM-DWI in the diagnosis of hepatic tumors. Studies have shown that^[6,52-58] IVIM-DWI can be used for the diagnosis and differentiation of benign and malignant hepatic tumours, and a consensus indicates that the ADC and D values have high efficacy for differential diagnosis. The D value is the only simple diffusion coefficient sensitive to water molecule diffusion. For malignant lesions characterized by diffusion restriction, the D value has higher diagnostic efficiency than the ADC^[54-56]. Lou *et al.*^[54] performed IVIM-DWI on 74 patients with hepatic tumors and showed that the ADC, D and f values in the malignant group were significantly lower than those in the benign group, with a larger area under the curve for the D value (0.968) and higher differentiation sensitivity (92.30%); however, no statistically significant difference in the D* value was found between the two groups. Furthermore, conflicting results have been reported^[53,57,59]. The results of the study by Watanabe *et al.*^[57] showed that for the identification of benign and malignant hepatic tumors, the area under the receiver operating characteristic (ROC) curve of the ADC value was higher than that of the D value; and Doblaz *et al.*^[59] suggested that compared with the ADC value, IVIM-DWI parameters could not improve the differentiation efficiency for hepatic focal lesions.

The use of the perfusion-related parameters D* and f for the differentiation of benign and malignant nodules is controversial^[58,60]. Penner AH *et al.*^[60] showed that compared with the traditional ADC, IVIM-DWI parameters were more significantly different between lesions and normal liver tissue. Ichikawa *et al.*^[58] studied 84 cases of focal benign and malignant hepatic lesions and found that the D and D* values of malignant hepatic lesions were significantly lower than those of benign hepatic lesions, while the f values showed no difference between benign and malignant hepatic lesions. These results suggested that the D* and D values were inhibited in malignant lesions. In contrast, some studies^[52-54,61] have suggested that the D* and f values are meaningless for differentiating benign and malignant hepatic lesions. A possible reason is that the D* value may fluctuate in a large range due to different blood supply types in hepatic hemangiomas^[52,61], while the magnitude of the f value depends on the time of echo (TE) (a longer TE corresponds to a greater f value). In addition, D* and f values are not uniquely specific to perfusion and may also be sensitive to other flow information, such as the excretion, direction or pattern of diffusion of a granule or gland^[53,57,62] (Figures 1 and 2, Table 2).

DIFFERENTIATION OF HEPATIC MALIGNANCIES WITH DIFFERENT PATHOLOGICAL TYPES

Few studies have investigated IVIM-DWI for the differentiation of hepatic malignancies of different pathological types. Previous studies have suggested that

Table 1 Summary of hepatic fibrosis intravoxel incoherent motion diffusion-weighted imaging studies

Ref.	Subject number	Key findings
Chen <i>et al</i> ^[45]	50	The ADC, D_{slow} , D_{fast} and FF values of liver fibrosis stages between the groups F0-1 and F2-4, and the groups F0-2 and F3-4 showed significant differences. As the stage of fibrosis increased, the values decreased
Hu <i>et al</i> ^[40]	57	Significant differences in D, f, D^* and ADC values were found between stages (stages F0-F4). Inverse correlations were identified between fibrosis stages and D, f, D^* , and ADC values
Ichikawa <i>et al</i> ^[41]	129	D^* , f and ADC values decreased with fibrosis stage
Wu <i>et al</i> ^[43]	49	Liver fibrosis exhibited significant correlations with D_{fast} and f values. D_{fast} values in the F4 group were significantly lower than those in the F0, F1 and F2 groups
Hu <i>et al</i> ^[39]	56	The mean, interquartile (IQ) range, and percentiles (50 th , 75 th and 90 th) of D^* maps were significantly different between the F0-1, F2-3 and F4 groups
Huang <i>et al</i> ^[48]	42	IVIM diffusion MRI has high diagnostic performance in detecting viral hepatitis B-induced liver fibrosis
Liang <i>et al</i> ^[49]	30	The D value decreased as the fibrosis level increased
Franca <i>et al</i> ^[50]	74	ADC and f values were lower with higher fibrosis stages

ADC: Apparent diffusion coefficient; IVIM: Intravoxel incoherent motion; MRI: Magnetic resonance imaging.

Table 2 Summary of hepatic nodules intravoxel incoherent motion diffusion-weighted imaging studies

Ref.	Subject number	Key findings
Luo <i>et al</i> ^[53]	27	ADC_{total} , D, and D^* values of HCC were lower than those of focal nodular hyperplasia
Luo <i>et al</i> ^[54]	75	ADC_{total} , D, and f values of malignant lesions were lower than those of benign lesions
Klauss <i>et al</i> ^[55]	72	D and ADC values of HCC were lower than those of focal nodular hyperplasia
Yoon <i>et al</i> ^[56]	157	True diffusion and ADC_{total} of malignancies were lower than those of benign malignant lesions
Watanabe <i>et al</i> ^[57]	120	D and ADC values were lower in the malignant group than in the benign group
Ichikawa <i>et al</i> ^[58]	84	D and D^* values of malignant lesions were lower than those of benign lesions
Doblas <i>et al</i> ^[59]	86	The apparent and pure diffusion coefficients were lower in malignant than in benign tumors
Penner <i>et al</i> ^[60]	61	ROC analysis demonstrated the best discriminability between HCCs and focal nodular hyperplasia for ADC_{slow} and f values
Zhu <i>et al</i> ^[61]	39	ADC_{total} and D values of malignancies were lower than those of hemangioma

ADC: Apparent diffusion coefficient; HCC: Hepatocellular carcinoma.

IVIM-DWI is beneficial for the differentiation of hepatocellular carcinoma (HCC) and intrahepatic cholangiocarcinoma (ICC)^[63-66], but the differentiation of HCC and metastatic hepatic cancer requires further study^[52]. Shao *et al*^[64] discussed the role of IVIM-DWI in differentiating hepatitis B virus (HBV)-related ICC from HCC and found that the ADC and D values of ICC were significantly higher than those of HCC, while the f value of ICC was significantly lower than that of HCC, and the areas under the ROC curves of the ADC, D and f values were 0.724, 0.753 and 0.741, respectively. Wei *et al*^[63] showed that the ADC and D value could differentiate ICC from HCC. However, the D^* and f values showed no difference in the ICC and HCC groups. Choi *et al*^[65] studied 161 cases of focal hepatic lesions using IVIM-DWI. The results showed no significant difference in the ADC value in any malignant tumor. The D_{slow} value of HCC was significantly lower than that of ICC, and the f value was significantly higher than those of ICC and metastatic carcinoma. A meta-analysis conducted by Wu *et al*^[52] (six papers meeting the requirements) showed that the ADC, D, D^* and f values were not significantly different between metastatic liver cancer and HCC. The reason for this finding may be that these metastases originated from some primary tumors such

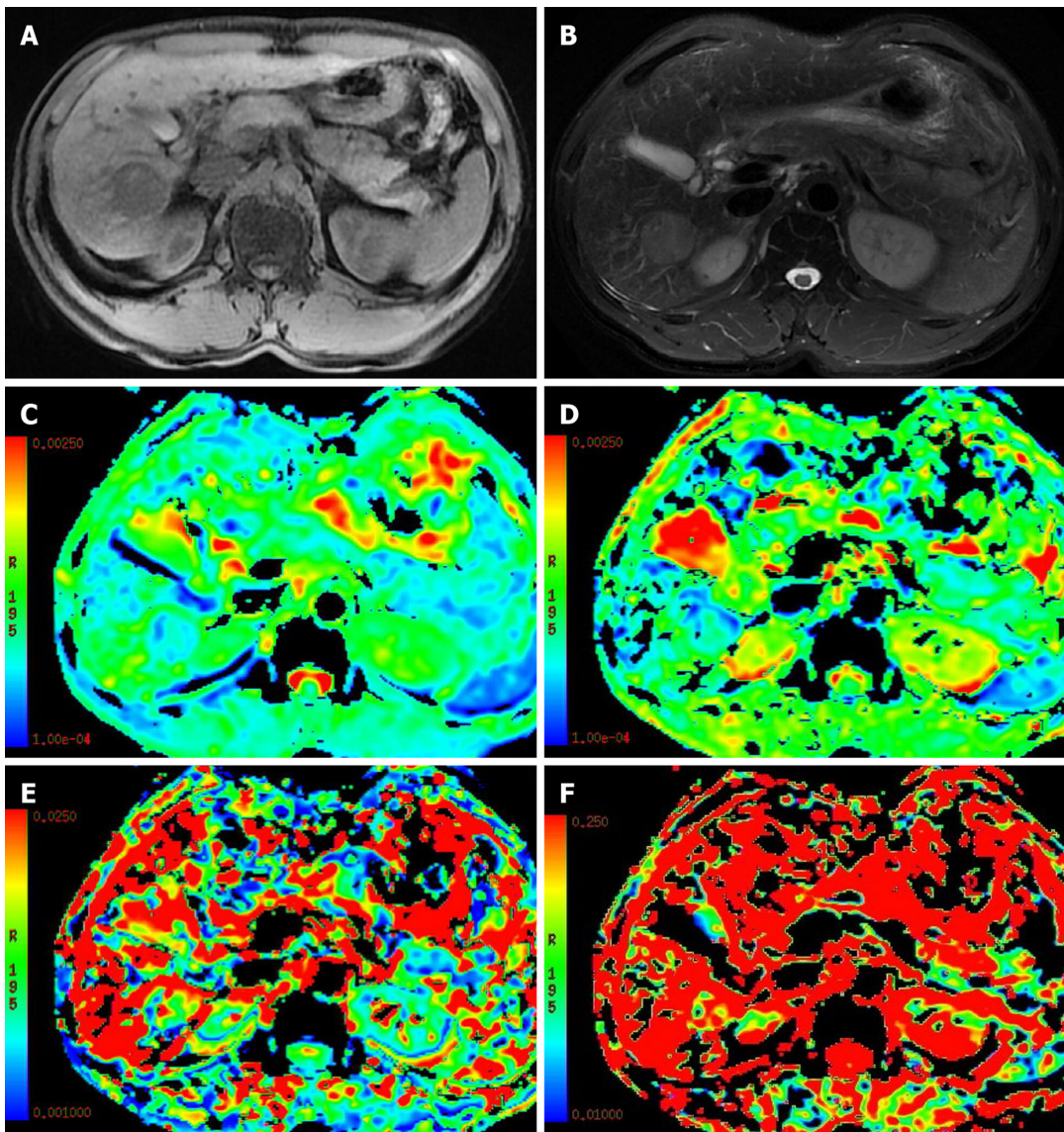


Figure 1 A 51-year-old male patient with hepatocellular carcinoma in the right lobe of the liver. The tumor was hypointense on T1-weighted image (T1WI) and hyperintense on T2-weighted image (T2WI). The apparent diffusion coefficient (ADC), D, D* and f maps were obtained by post processing of IVIM-DWI images. A: T1WI; B: T2WI; C: ADC map; D: D map; E: D* map; F: F map.

as lesions in the gastrointestinal tract, lung, breast or urogenital system, which may have caused some changes in cell density and microcirculation. In addition, different HCC histological classifications and compositions used in different studies may have also caused certain effects.

HCC HISTOLOGICAL CLASSIFICATION

Studies have shown that the IVIM-DWI parameters of HCC are correlated with histological classification^[19,67-75]. Li *et al*^[73] performed an IVIM-DWI analysis on a rat model of hepatic cancer and showed that the ADC and D values of higher-grade lesions were lower than those of lower-grade lesions, and the ADC and D values were negatively correlated with the tumor's histological classification. The D* and f values of higher-grade lesions were higher than those of lower-grade lesions, and the D* and f values were positively correlated with the tumor histological classification. During tumorigenesis, as the degree of tumor differentiation becomes increasingly poor, the cellularity and nuclear-to-cytoplasmic ratio increase, and as the extracellular space decreases, water diffusion is restricted, resulting in reduced ADC and D values in poorly differentiated HCC^[68,69].

Regarding the role of D* and f values in the histological classification of HCC, the

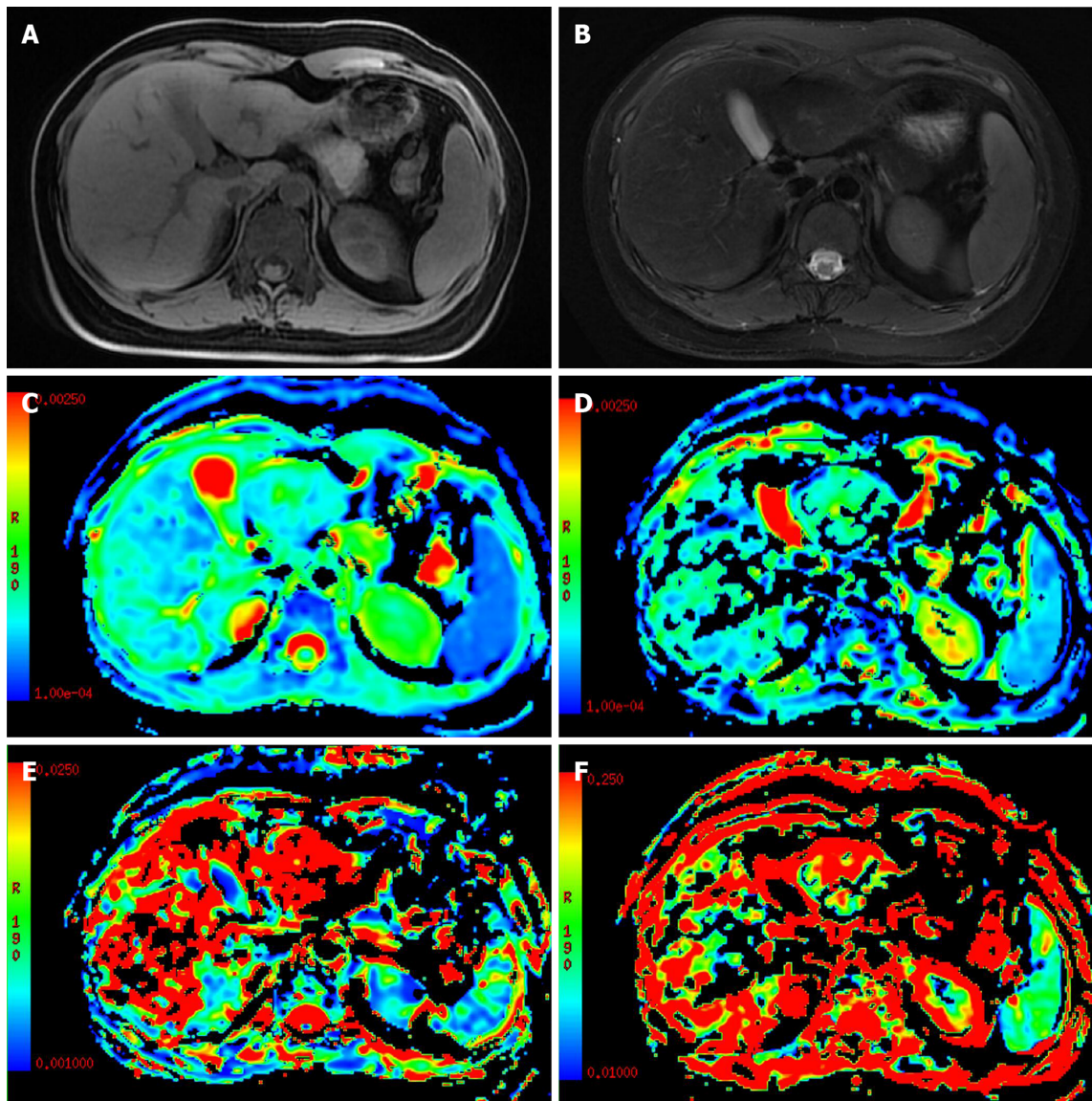


Figure 2 A 28-year-old female patient with focal nodular hyperplasia in the left lobe of the liver. The tumor was isointense on T1-weighted image (T1WI) and T2-weighted image (T2WI) with a star-shaped area in the center of the lesion (hypointense on T1WI and hyperintense on T2WI). A: T1WI; B: T2WI; C: ADC map; D: D map; E: D* map; F: f map.

results of available studies are not completely consistent. Sokmen *et al*^[71] showed that the ADC and D values were negatively correlated with the histological classification of HCC, the f value was positively correlated with the histological classification of HCC tissue, and no differences in the D* value in different histological classifications of HCC were observed. Granata *et al*^[74,75] observed the role of the ADC, D and f values in differentiating the histological classifications of HCC but did not observe any significance of the D* value for differentiation. Other studies showed only the roles of the ADC and D value in the differentiation of the histological classifications of HCC, and the roles of D* and f values in differentiation were not observed^[19,67-69], which may be explained by differences in b-value groupings and patient populations as well as consequent variation in tumor grade distributions^[67,75].

EVALUATION OF THE HCC TREATMENT RESPONSE

Studies have shown that IVIM-DWI has important application value in the treatment and follow-up of HCC.

Zhang *et al*^[76] conducted IVIM-DWI on 157 patients with HBV-related HCC who underwent surgical resection. The results showed 47 cases of tumor recurrence, and a D value $< 0.985 \times 10^{-3} \text{ mm}^2/\text{s}$ was found to be a risk factor for recurrence. The D value

of the IVIM-DWI model has been suggested as a potential biomarker for preoperative prediction of hepatic cancer recurrence^[77-79]. Zhao *et al.*^[78] reported that D is an independent predictor of microvascular invasion (MVI); when the cut-off D value was 1.16×10^{-3} mm²/s, the sensitivity and specificity for predicting MVI were 66.7% and 88.9, respectively.

IVIM-DWI parameters can distinguish the survival area, the fibrous area and the necrotic area of malignant hepatic tumors^[80]. A study^[81] including 15 patients undergoing resection of hepatic metastases of colorectal cancer found that the ADC and D values were associated with the degree of necrosis of metastatic hepatic tumors, suggesting that the specificity of free molecular proliferation of metastatic colorectal cancer increased after systemic chemotherapy.

In the early stages of local or targeted therapy for tumors, changes in tumor volume are often not detected by traditional imaging, and functional imaging is of great value in this field^[82,83]. IVIM-DWI parameters can be used as biomarkers for early response evaluation^[84-88]. Studies have shown that IVIM-DWI has important value in the evaluation of transarterial chemoembolization (TACE) treatment responses and the prediction of therapeutic effects in HCC^[84,89-93]. The study by Peng *et al.*^[91] showed that after TACE treatment for HCC, the ADC and D values in tumor tissues significantly increased, the D* value decreased significantly, and the f value did not change significantly. The reason for the inconsistent changes in these two perfusion-related parameters may be that the D* and f values represent different aspects of perfusion, the former is mainly related to the capillary velocity of local tissues, while the latter is related to the blood volume of local tissues. The study by Park *et al.*^[89] showed that the D* value could reflect the blood supply of HCC and predict the deposition effect of iodide oil after TACE surgery; the D* value and arterial enhancement ratio (AER) of preoperative lesions in the group with better iodized oil deposition were significantly higher than those in the group with poor iodized oil deposition. Wu *et al.*^[92] believed that the ADC maybe the best independent predictor of TACE treatment responses.

The IVIM-DWI perfusion parameter f is significantly correlated with microvascular dysplasia (MVD) in HCC^[88]. IVIM-DWI can be used to evaluate the anti-angiogenic effect of sorafenib on HCC^[87,88,94-96]. Yang *et al.*^[95] established 35 nude mouse models of HCC and conducted IVIM-DWI at baseline and 7, 14 and 21 days after sorafenib treatment. The results revealed that compared with the control group, the ADC and D values in the treatment group at each time point were significantly increased, while the f value was significantly decreased at 7 days and significantly increased at 21 days. In the treatment group, both the ADC and D values were significantly higher than the baseline values on days 7, 14 and 21, while the f value decreased significantly on the 7th day and increased significantly on the 21st day. In the treatment group, the ADC, D and f values were significantly correlated with the necrotic fraction (NF). These results suggested that IVIM-DWI parameters can be used as biomarkers to evaluate the therapeutic efficacy of sorafenib therapy for HCC. Shirota *et al.*^[97] conducted IVIM-DWI on nine patients with HCC treated with sorafenib, and the results showed that the baseline D value in the responsive group was significantly higher than that in the non-responsive group. The sensitivity and specificity of the differential therapeutic responses were 100% and 67%, respectively, and the other parameters showed no difference between the two groups, suggesting that the D value can be used to predict the therapeutic response of HCC to sorafenib.

OTHER DISEASES

The application of IVIM-DWI in hepatic ischemia-reperfusion injury (IRI)^[97-99], hepatic alveolar echinococcosis^[100], hepatic dysfunction^[101], hepatic sinus obstruction syndrome^[102] and other diseases is also gradually developing. For example, studies have found that IVIM-DWI-related parameters are significantly reduced after liver IRI^[99].

CONCLUSION

In conclusion, IVIM-DWI seems to accurately reflect information related to the diffusion of simple water molecules and microcirculatory perfusion in tissues and it could have important application value in the diagnosis of hepatic fibrosis, the differentiation of benign and malignant hepatic lesions, the histological classification of HCC, the evaluation of local and targeted therapeutic response and the prediction

of therapeutic efficacy. However, the value of IVIM-DWI in assisting in the histological classification of hepatic fibrosis and in differentiating malignant hepatic tumors with different pathological characteristics still requires further investigation. The standardization of IVIM-DWI scanning technology (such as the optimization and standardization of the number and distribution of b values) is an important topic, which warrants further study. In addition, the characteristics and diagnostic value of the D^* and f values still require further exploration. With continuous innovation in IVIM-DWI technology and in-depth clinical research, IVIM-DWI will play a more important role in the diagnosis and treatment of hepatic diseases in the future.

REFERENCES

- 1 **Taouli B**, Koh DM. Diffusion-weighted MR imaging of the liver. *Radiology* 2010; **254**: 47-66 [PMID: 20032142 DOI: 10.1148/radiol.09090021]
- 2 **Bammer R**. Basic principles of diffusion-weighted imaging. *Eur J Radiol* 2003; **45**: 169-184 [PMID: 12595101 DOI: 10.1016/s0720-048x(02)00303-0]
- 3 **Lewis S**, Dyvorne H, Cui Y, Taouli B. Diffusion-weighted imaging of the liver: techniques and applications. *MagnReson Imaging Clin N Am* 2014; **22**: 373-395 [PMID: 25086935 DOI: 10.1016/j.mric.2014.04.009]
- 4 **Le Bihan D**, Breton E, Lallemand D, Aubin ML, Vignaud J, Laval-Jeantet M. Separation of diffusion and perfusion in intravoxel incoherent motion MR imaging. *Radiology* 1988; **168**: 497-505 [PMID: 3393671 DOI: 10.1148/radiology.168.2.3393671]
- 5 **Le Bihan D**, Breton E, Lallemand D, Grenier P, Cabanis E, Laval-Jeantet M. MR imaging of intravoxel incoherent motions: application to diffusion and perfusion in neurologic disorders. *Radiology* 1986; **161**: 401-407 [PMID: 3763909 DOI: 10.1148/radiology.161.2.3763909]
- 6 **Yamada I**, Aung W, Himeno Y, Nakagawa T, Shibuya H. Diffusion coefficients in abdominal organs and hepatic lesions: evaluation with intravoxel incoherent motion echo-planar MR imaging. *Radiology* 1999; **210**: 617-623 [PMID: 10207458 DOI: 10.1148/radiology.210.3.r99fe17617]
- 7 **Federau C**. Intravoxel incoherent motion MRI as a means to measure in vivo perfusion: A review of the evidence. *NMR Biomed* 2017; **30** [PMID: 28885745 DOI: 10.1002/nbm.3780]
- 8 **Paschoal AM**, Leoni RF, Dos Santos AC, Paiva FF. Intravoxel incoherent motion MRI in neurological and cerebrovascular diseases. *Neuroimage Clin* 2018; **20**: 705-714 [PMID: 30221622 DOI: 10.1016/j.nicl.2018.08.030]
- 9 **Luciani A**, Vignaud A, Cavet M, Nhieu JT, Mallat A, Ruel L, Laurent A, Deux JF, Brugieres P, Rahmouni A. Liver cirrhosis: intravoxel incoherent motion MR imaging--pilot study. *Radiology* 2008; **249**: 891-899 [PMID: 19011186 DOI: 10.1148/radiol.2493080080]
- 10 **Bisdas S**, Braun C, Skardelly M, Schittenhelm J, Teo TH, Thng CH, Klose U, Koh TS. Correlative assessment of tumor microcirculation using contrast-enhanced perfusion MRI and intravoxel incoherent motion diffusion-weighted MRI: is there a link between them? *NMR Biomed* 2014; **27**: 1184-1191 [PMID: 25088433 DOI: 10.1002/nbm.3172]
- 11 **Dyvorne H**, Jajamovich G, Kakite S, Kuehn B, Taouli B. Intravoxel incoherent motion diffusion imaging of the liver: optimal b-value subsampling and impact on parameter precision and reproducibility. *Eur J Radiol* 2014; **83**: 2109-2113 [PMID: 25277521 DOI: 10.1016/j.ejrad.2014.09.003]
- 12 **Patel J**, Sigmund EE, Rusinek H, Oei M, Babb JS, Taouli B. Diagnosis of cirrhosis with intravoxel incoherent motion diffusion MRI and dynamic contrast-enhanced MRI alone and in combination: preliminary experience. *J MagnReson Imaging* 2010; **31**: 589-600 [PMID: 20187201 DOI: 10.1002/jmri.22081]
- 13 **Cohen AD**, Schieke MC, Hohenwarter MD, Schmainda KM. The effect of low b-values on the intravoxel incoherent motion derived pseudodiffusion parameter in liver. *MagnReson Med* 2015; **73**: 306-311 [PMID: 24478175 DOI: 10.1002/mrm.25109]
- 14 **Koh DM**, Collins DJ, Orton MR. Intravoxel incoherent motion in body diffusion-weighted MRI: reality and challenges. *AJR Am J Roentgenol* 2011; **196**: 1351-1361 [PMID: 21606299 DOI: 10.2214/AJR.10.5515]
- 15 **Jalnefjord O**, Montelius M, Starck G, Ljungberg M. Optimization of b-value schemes for estimation of the diffusion coefficient and the perfusion fraction with segmented intravoxel incoherent motion model fitting. *MagnReson Med* 2019; **82**: 1541-1552 [PMID: 31148264 DOI: 10.1002/mrm.27826]
- 16 **Mürtz P**, Sprinkart AM, Reick M, Pieper CC, Schievelkamp AH, König R, Schild HH, Willinek WA, Kukuk GM. Accurate IVIM model-based liver lesion characterisation can be achieved with only three b-value DWI. *EurRadiol* 2018; **28**: 4418-4428 [PMID: 29671057 DOI: 10.1007/s00330-018-5401-7]
- 17 **Meeus EM**, Novak J, Dehghani H, Peet AC. Rapid measurement of intravoxel incoherent motion (IVIM) derived perfusion fraction for clinical magnetic resonance imaging. *MAGMA* 2018; **31**: 269-283 [PMID: 29075909 DOI: 10.1007/s10334-017-0656-6]
- 18 **Wong OL**, Goh Lo G, Yuan J, Chung WK, Ho WHB, Noseworthy MD. Evaluation and Minimization of the Pseudohepatic Anisotropy Artifact in Liver Intravoxel Incoherent Motion. *J Comput Assist Tomogr* 2017; **41**: 679-687 [PMID: 28708735 DOI: 10.1097/RCT.0000000000000604]
- 19 **Dyvorne HA**, Galea N, Nevers T, Fiel MI, Carpenter D, Wong E, Orton M, de Oliveira A, Feiweier T, Vachon ML, Babb JS, Taouli B. Diffusion-weighted imaging of the liver with multiple b values: effect of diffusion gradient polarity and breathing acquisition on image quality and intravoxel incoherent motion parameters--a pilot study. *Radiology* 2013; **266**: 920-929 [PMID: 23220895 DOI: 10.1148/radiol.12120686]
- 20 **Xiang Z**, Ai Z, Liang J, Li G, Zhu X, Yan X. Evaluation of Regional Variability and Measurement Reproducibility of Intravoxel Incoherent Motion Diffusion Weighted Imaging Using a Cardiac Stationary Phase Based ECG Trigger Method. *Biomed Res Int* 2018; **2018**: 4604218 [PMID: 29850518 DOI: 10.1080/17445019.2018.1533333]

- 10.1155/2018/4604218]
- 21 **Li J**, Zhang C, Cui Y, Liu H, Chen W, Wang G, Wang D. Intravoxel incoherent motion diffusion-weighted MR imaging of the liver using respiratory-cardiac double triggering. *Oncotarget* 2017; **8**: 94959-94968 [PMID: 29212282 DOI: 10.18632/oncotarget.21824]
 - 22 **Neil JJ**, Bretthorst GL. On the use of Bayesian probability theory for analysis of exponential decay data: an example taken from intravoxel incoherent motion experiments. *MagnReson Med* 1993; **29**: 642-647 [PMID: 8505900 DOI: 10.1002/mrm.1910290510]
 - 23 **Ahn SJ**, Shin HJ, Chang JH, Lee SK. Differentiation between primary cerebral lymphoma and glioblastoma using the apparent diffusion coefficient: comparison of three different ROI methods. *PLoS One* 2014; **9**: e112948 [PMID: 25393543 DOI: 10.1371/journal.pone.0112948]
 - 24 **Blazic IM**, Lilic GB, Gajic MM. Quantitative Assessment of Rectal Cancer Response to Neoadjuvant Combined Chemotherapy and Radiation Therapy: Comparison of Three Methods of Positioning Region of Interest for ADC Measurements at Diffusion-weighted MR Imaging. *Radiology* 2017; **282**: 418-428 [PMID: 27253423 DOI: 10.1148/radiol.2016151908]
 - 25 **Nougaret S**, Vargas HA, Lakhman Y, Sudre R, Do RK, Bibeau F, Azria D, Assenat E, Molinari N, Pierredon MA, Rouanet P, Guiu B. Intravoxel Incoherent Motion-derived Histogram Metrics for Assessment of Response after Combined Chemotherapy and Radiation Therapy in Rectal Cancer: Initial Experience and Comparison between Single-Section and Volumetric Analyses. *Radiology* 2016; **280**: 446-454 [PMID: 26919562 DOI: 10.1148/radiol.2016150702]
 - 26 **Giordano M**, Samii A, Samii M, Nabavi A. Magnetic Resonance Imaging-Apparent Diffusion Coefficient Assessment of Vestibular Schwannomas: Systematic Approach, Methodology, and Pitfalls. *World Neurosurg* 2019; **125**: e820-e823 [PMID: 30738940 DOI: 10.1016/j.wneu.2019.01.176]
 - 27 **Wang S**, Meng M, Zhang X, Wu C, Wang R, Wu J, Sami MU, Xu K. Texture analysis of diffusion weighted imaging for the evaluation of glioma heterogeneity based on different regions of interest. *Oncol Lett* 2018; **15**: 7297-7304 [PMID: 29731887 DOI: 10.3892/ol.2018.8232]
 - 28 **Ahlawat S**, Khandheria P, Del Grande F, Morelli J, Subhawong TK, Demehri S, Fayad LM. Interobserver variability of selective region-of-interest measurement protocols for quantitative diffusion weighted imaging in soft tissue masses: Comparison with whole tumor volume measurements. *J MagnReson Imaging* 2016; **43**: 446-454 [PMID: 26174705 DOI: 10.1002/jmri.24994]
 - 29 **Chalasanani N**, Younossi Z, Lavine JE, Diehl AM, Brunt EM, Cusi K, Charlton M, Sanyal AJ. The diagnosis and management of non-alcoholic fatty liver disease: practice Guideline by the American Association for the Study of Liver Diseases, American College of Gastroenterology, and the American Gastroenterological Association. *Hepatology* 2012; **55**: 2005-2023 [PMID: 22488764 DOI: 10.1002/hep.25762]
 - 30 **Murphy P**, Hooker J, Ang B, Wolfson T, Gamst A, Bydder M, Middleton M, Peterson M, Behling C, Loomba R, Sirlin C. Associations between histologic features of nonalcoholic fatty liver disease (NAFLD) and quantitative diffusion-weighted MRI measurements in adults. *J MagnReson Imaging* 2015; **41**: 1629-1638 [PMID: 25256692 DOI: 10.1002/jmri.24755]
 - 31 **Parente DB**, Paiva FF, Oliveira Neto JA, Machado-Silva L, Figueiredo FA, Lanzoni V, Campos CF, do Brasil PE, Gomes Mde B, Perez Rde M, Rodrigues RS. Intravoxel Incoherent Motion Diffusion Weighted MR Imaging at 3.0 T: Assessment of Steatohepatitis and Fibrosis Compared with Liver Biopsy in Type 2 Diabetic Patients. *PLoS One* 2015; **10**: e0125653 [PMID: 25961735 DOI: 10.1371/journal.pone.0125653]
 - 32 **Shin HJ**, Yoon H, Kim MJ, Han SJ, Koh H, Kim S, Lee MJ. Liver intravoxel incoherent motion diffusion-weighted imaging for the assessment of hepatic steatosis and fibrosis in children. *World J Gastroenterol* 2018; **24**: 3013-3020 [PMID: 30038468 DOI: 10.3748/wjg.v24.i27.3013]
 - 33 **Guiu B**, Petit JM, Capitan V, Aho S, Masson D, Lefevre PH, Favelier S, Loffroy R, Vergès B, Hillon P, Krausé D, Cercueil JP. Intravoxel incoherent motion diffusion-weighted imaging in nonalcoholic fatty liver disease: a 3.0-T MR study. *Radiology* 2012; **265**: 96-103 [PMID: 22843768 DOI: 10.1148/radiol.12112478]
 - 34 **Joo I**, Lee JM, Yoon JH, Jang JJ, Han JK, Choi BI. Nonalcoholic fatty liver disease: intravoxel incoherent motion diffusion-weighted MR imaging-an experimental study in a rabbit model. *Radiology* 2014; **270**: 131-140 [PMID: 24091358 DOI: 10.1148/radiol.13122506]
 - 35 **Yoon JH**, Lee JM, Lee KB, Kim D, Kabasawa H, Han JK. Comparison of monoexponential, intravoxel incoherent motion diffusion-weighted imaging and diffusion kurtosis imaging for assessment of hepatic fibrosis. *ActaRadiol* 2019; **60**: 1593-1601 [PMID: 30935212 DOI: 10.1177/0284185119840219]
 - 36 **Shiraga K**, Ono K, Inuzuka R, Asakai H, Ookubo T, Shirayama A, Higashi K, Nakajima H. Intravoxel incoherent motion imaging has the possibility to detect liver abnormalities in young Fontan patients with good hemodynamics. *Cardiol Young* 2019; **29**: 898-903 [PMID: 31250776 DOI: 10.1017/S1047951119001070]
 - 37 **Tosun M**, Onal T, Uslu H, Alparslan B, ÇetinAkhan S. Intravoxel incoherent motion imaging for diagnosing and staging the liver fibrosis and inflammation. *AbdomRadiol (NY)* 2020; **45**: 15-23 [PMID: 31705248 DOI: 10.1007/s00261-019-02300-z]
 - 38 **Wáng YXJ**, Deng M, Li YT, Huang H, Leung JCS, Chen W, Lu PX. A Combined Use of Intravoxel Incoherent Motion MRI Parameters Can Differentiate Early-Stage Hepatitis-b Fibrotic Livers from Healthy Livers. *SLAS Technol* 2018; **23**: 259-268 [PMID: 28666091 DOI: 10.1177/2472630317717049]
 - 39 **Hu F**, Yang R, Huang Z, Wang M, Zhang H, Yan X, Song B. Liver fibrosis: in vivo evaluation using intravoxel incoherent motion-derived histogram metrics with histopathologic findings at 3.0 T. *AbdomRadiol (NY)* 2017; **42**: 2855-2863 [PMID: 28624925 DOI: 10.1007/s00261-017-1208-2]
 - 40 **Hu G**, Chan Q, Quan X, Zhang X, Li Y, Zhong X, Lin X. Intravoxel incoherent motion MRI evaluation for the staging of liver fibrosis in a rat model. *J MagnReson Imaging* 2015; **42**: 331-339 [PMID: 25384923 DOI: 10.1002/jmri.24796]
 - 41 **Ichikawa S**, Motosugi U, Morisaka H, Sano K, Ichikawa T, Enomoto N, Matsuda M, Fujii H, Onishi H. MRI-based staging of hepatic fibrosis: Comparison of intravoxel incoherent motion diffusion-weighted imaging with magnetic resonance elastography. *J MagnReson Imaging* 2015; **42**: 204-210 [PMID: 25223820 DOI: 10.1002/jmri.24760]
 - 42 **Chung SR**, Lee SS, Kim N, Yu ES, Kim E, Kühn B, Kim IS. Intravoxel incoherent motion MRI for liver

- fibrosis assessment: a pilot study. *ActaRadiol* 2015; **56**: 1428-1436 [PMID: 25414372 DOI: 10.1177/0284185114559763]
- 43 **Wu CH**, Ho MC, Jeng YM, Liang PC, Hu RH, Lai HS, Shih TT. Assessing hepatic fibrosis: comparing the intravoxel incoherent motion in MRI with acoustic radiation force impulse imaging in US. *EurRadiol* 2015; **25**: 3552-3559 [PMID: 25991478 DOI: 10.1007/s00330-015-3774-4]
- 44 **Lu PX**, Huang H, Yuan J, Zhao F, Chen ZY, Zhang Q, Ahuja AT, Zhou BP, Wang YX. Decreases in molecular diffusion, perfusion fraction and perfusion-related diffusion in fibrotic livers: a prospective clinical intravoxel incoherent motion MR imaging study. *PLoS One* 2014; **9**: e113846 [PMID: 25436458 DOI: 10.1371/journal.pone.0113846]
- 45 **Chen C**, Wang B, Shi D, Fu F, Zhang J, Wen Z, Zhu S, Xu J, Lin Q, Li J, Dou S. Initial study of biexponential model of intravoxel incoherent motion magnetic resonance imaging in evaluation of the liver fibrosis. *Chin Med J (Engl)* 2014; **127**: 3082-3087 [PMID: 25189949]
- 46 **Zhang Y**, Jin N, Deng J, Guo Y, White SB, Yang GY, Omary RA, Larson AC. Intra-voxel incoherent motion MRI in rodent model of diethylnitrosamine-induced liver fibrosis. *MagnReson Imaging* 2013; **31**: 1017-1021 [PMID: 23598061 DOI: 10.1016/j.mri.2013.03.007]
- 47 **Hayashi T**, Miyati T, Takahashi J, Fukuzawa K, Sakai H, Tano M, Saitoh S. Diffusion analysis with triexponential function in liver cirrhosis. *J MagnReson Imaging* 2013; **38**: 148-153 [PMID: 23239543 DOI: 10.1002/jmri.23966]
- 48 **Huang H**, Che-Nordin N, Wang LF, Xiao BH, Chevallier O, Yun YX, Guo SW, Wang YXJ. High performance of intravoxel incoherent motion diffusion MRI in detecting viral hepatitis-b induced liver fibrosis. *Ann Transl Med* 2019; **7**: 39 [PMID: 30906743 DOI: 10.21037/atm.2018.12.33]
- 49 **Liang J**, Song X, Xiao Z, Chen H, Shi C, Luo L. Using IVIM-MRI and R2 \square Mapping to Differentiate Early Stage Liver Fibrosis in a Rat Model of Radiation-Induced Liver Fibrosis. *Biomed Res Int* 2018; **2018**: 4673814 [PMID: 30627558 DOI: 10.1155/2018/4673814]
- 50 **França M**, Martí-Bonmatí L, Alberich-Bayarri Á, Oliveira P, Guimaraes S, Oliveira J, Amorim J, Gonzalez JS, Vizcaino JR, Miranda HP. Evaluation of fibrosis and inflammation in diffuse liver diseases using intravoxel incoherent motion diffusion-weighted MR imaging. *AbdomRadiol (NY)* 2017; **42**: 468-477 [PMID: 27638516 DOI: 10.1007/s00261-016-0899-0]
- 51 **Yoon JH**, Lee JM, Baek JH, Shin CI, Kiefer B, Han JK, Choi BI. Evaluation of hepatic fibrosis using intravoxel incoherent motion in diffusion-weighted liver MRI. *J Comput Assist Tomogr* 2014; **38**: 110-116 [PMID: 24378888 DOI: 10.1097/RCT.0b013e3182a589be]
- 52 **Wu H**, Liang Y, Jiang X, Wei X, Liu Y, Liu W, Guo Y, Tang W. Meta-analysis of intravoxel incoherent motion magnetic resonance imaging in differentiating focal lesions of the liver. *Medicine (Baltimore)* 2018; **97**: e12071 [PMID: 30142864 DOI: 10.1097/MD.00000000000012071]
- 53 **Luo M**, Zhang L, Jiang XH, Zhang WD. Intravoxel incoherent motion: application in differentiation of hepatocellular carcinoma and focal nodular hyperplasia. *DiagnIntervRadiol* 2017; **23**: 263-271 [PMID: 28703102 DOI: 10.5152/dir.2017.16595]
- 54 **Luo M**, Zhang L, Jiang XH, Zhang WD. Intravoxel Incoherent Motion Diffusion-weighted Imaging: Evaluation of the Differentiation of Solid Hepatic Lesions. *TranslOncol* 2017; **10**: 831-838 [PMID: 28866259 DOI: 10.1016/j.tranon.2017.08.003]
- 55 **Klauss M**, Mayer P, Maier-Hein K, Laun FB, Mehrabi A, Kauczor HU, Stieltjes B. IVIM-diffusion-MRI for the differentiation of solid benign and malign hypervascular liver lesions-Evaluation with two different MR scanners. *Eur J Radiol* 2016; **85**: 1289-1294 [PMID: 27235876 DOI: 10.1016/j.ejrad.2016.04.011]
- 56 **Yoon JH**, Lee JM, Yu MH, Kiefer B, Han JK, Choi BI. Evaluation of hepatic focal lesions using diffusion-weighted MR imaging: comparison of apparent diffusion coefficient and intravoxel incoherent motion-derived parameters. *J MagnReson Imaging* 2014; **39**: 276-285 [PMID: 23633178 DOI: 10.1002/jmri.24158]
- 57 **Watanabe H**, Kanematsu M, Goshima S, Kajita K, Kawada H, Noda Y, Tatabashi Y, Kawai N, Kondo H, Moriyama N. Characterizing focal hepatic lesions by free-breathing intravoxel incoherent motion MRI at 3.0 T. *ActaRadiol* 2014; **55**: 1166-1173 [PMID: 24316660 DOI: 10.1177/0284185113514966]
- 58 **Ichikawa S**, Motosugi U, Ichikawa T, Sano K, Morisaka H, Araki T. Intravoxel incoherent motion imaging of focal hepatic lesions. *J MagnReson Imaging* 2013; **37**: 1371-1376 [PMID: 23172819 DOI: 10.1002/jmri.23930]
- 59 **Doblas S**, Wagner M, Leitao HS, Daire JL, Sinkus R, Vilgrain V, Van Beers BE. Determination of malignancy and characterization of hepatic tumor type with diffusion-weighted magnetic resonance imaging: comparison of apparent diffusion coefficient and intravoxel incoherent motion-derived measurements. *Invest Radiol* 2013; **48**: 722-728 [PMID: 23669588 DOI: 10.1097/RLI.0b013e3182915912]
- 60 **Penner AH**, Sprinkart AM, Kukuk GM, Gütgemann I, Gieseke J, Schild HH, Willinek WA, Mürtz P. Intravoxel incoherent motion model-based liver lesion characterisation from three b-value diffusion-weighted MRI. *EurRadiol* 2013; **23**: 2773-2783 [PMID: 23666233 DOI: 10.1007/s00330-013-2869-z]
- 61 **Zhu L**, Cheng Q, Luo W, Bao L, Guo G. A comparative study of apparent diffusion coefficient and intravoxel incoherent motion-derived parameters for the characterization of common solid hepatic tumors. *ActaRadiol* 2015; **56**: 1411-1418 [PMID: 25422515 DOI: 10.1177/0284185114559426]
- 62 **Shinmoto H**, Tamura C, Soga S, Shiomi E, Yoshihara N, Kaji T, Mulkern RV. An intravoxel incoherent motion diffusion-weighted imaging study of prostate cancer. *AJR Am J Roentgenol* 2012; **199**: W496-W500 [PMID: 22997399 DOI: 10.2214/AJR.11.8347]
- 63 **Wei Y**, Gao F, Zheng D, Huang Z, Wang M, Hu F, Chen C, Duan T, Chen J, Cao L, Song B. Intrahepatic cholangiocarcinoma in the setting of HBV-related cirrhosis: Differentiation with hepatocellular carcinoma by using Intravoxel incoherent motion diffusion-weighted MR imaging. *Oncotarget* 2018; **9**: 7975-7983 [PMID: 29487707 DOI: 10.18632/oncotarget.23807]
- 64 **Shao S**, Shan Q, Zheng N, Wang B, Wang J. Role of Intravoxel Incoherent Motion in Discriminating Hepatitis B Virus-Related Intrahepatic Mass-Forming Cholangiocarcinoma from Hepatocellular Carcinoma Based on Liver Imaging Reporting and Data System v2018. *Cancer BiotherRadiopharm* 2019; **34**: 511-518 [PMID: 31314589 DOI: 10.1089/cbr.2019.2799]
- 65 **Choi IY**, Lee SS, Sung YS, Cheong H, Lee H, Byun JH, Kim SY, Lee SJ, Shin YM, Lee MG. Intravoxel

- incoherent motion diffusion-weighted imaging for characterizing focal hepatic lesions: Correlation with lesion enhancement. *J Magn Reson Imaging* 2017; **45**: 1589-1598 [PMID: 27664970 DOI: 10.1002/jmri.25492]
- 66 Peng J, Zheng J, Yang C, Wang R, Zhou Y, Tao YY, Gong XQ, Wang WC, Zhang XM, Yang L. Intravoxel incoherent motion diffusion-weighted imaging to differentiate hepatocellular carcinoma from intrahepatic cholangiocarcinoma. *Sci Rep* 2020; **10**: 7717 [PMID: 32382050 DOI: 10.1038/s41598-020-64804-9]
- 67 Woo S, Lee JM, Yoon JH, Joo I, Han JK, Choi BI. Intravoxel incoherent motion diffusion-weighted MR imaging of hepatocellular carcinoma: correlation with enhancement degree and histologic grade. *Radiology* 2014; **270**: 758-767 [PMID: 24475811 DOI: 10.1148/radiol.13130444]
- 68 Zhu SC, Liu YH, Wei Y, Li LL, Dou SW, Sun TY, Shi DP. Intravoxel incoherent motion diffusion-weighted magnetic resonance imaging for predicting histological grade of hepatocellular carcinoma: Comparison with conventional diffusion-weighted imaging. *World J Gastroenterol* 2018; **24**: 929-940 [PMID: 29491686 DOI: 10.3748/wjg.v24.i8.929]
- 69 Wei Y, Gao F, Wang M, Huang Z, Tang H, Li J, Wang Y, Zhang T, Wei X, Zheng D, Song B. Intravoxel incoherent motion diffusion-weighted imaging for assessment of histologic grade of hepatocellular carcinoma: comparison of three methods for positioning region of interest. *Eur Radiol* 2019; **29**: 535-544 [PMID: 30027411 DOI: 10.1007/s00330-018-5638-1]
- 70 Yang D, She H, Wang X, Yang Z, Wang Z. Diagnostic accuracy of quantitative diffusion parameters in the pathological grading of hepatocellular carcinoma: A meta-analysis. *J Magn Reson Imaging* 2020; **51**: 1581-1593 [PMID: 31654537 DOI: 10.1002/jmri.26963]
- 71 Sokmen BK, Sabet S, Oz A, Server S, Namal E, Dayangac M, Dogusoy GB, Tokat Y, Inan N. Value of Intravoxel Incoherent Motion for Hepatocellular Carcinoma Grading. *Transplant Proc* 2019; **51**: 1861-1866 [PMID: 31399170 DOI: 10.1016/j.transproceed.2019.02.027]
- 72 Ichikawa S, Motosugi U, Hernando D, Morisaka H, Enomoto N, Matsuda M, Onishi H. Histological Grading of Hepatocellular Carcinomas with Intravoxel Incoherent Motion Diffusion-weighted Imaging: Inconsistent Results Depending on the Fitting Method. *Magn Reson Med Sci* 2018; **17**: 168-173 [PMID: 28819085 DOI: 10.2463/mrms.mp.2017-0047]
- 73 Li M, Zheng XJ, Huang ZX, Song B. [Predicting Histological Grade of HCC in Rats using Intravoxel Incoherent Motion Imaging]. *Sichuan Da Xue Xue Bao Yi Xue Ban* 2018; **49**: 243-247 [PMID: 29737069]
- 74 Granata V, Fusco R, Filice S, Catalano O, Piccirillo M, Palaia R, Izzo F, Petrillo A. The current role and future perspectives of functional parameters by diffusion weighted imaging in the assessment of histologic grade of HCC. *Infect Agent Cancer* 2018; **13**: 23 [PMID: 29988667 DOI: 10.1186/s13027-018-0194-5]
- 75 Granata V, Fusco R, Catalano O, Guarino B, Granata F, Tatangelo F, Avallone A, Piccirillo M, Palaia R, Izzo F, Petrillo A. Intravoxel incoherent motion (IVIM) in diffusion-weighted imaging (DWI) for Hepatocellular carcinoma: correlation with histologic grade. *Oncotarget* 2016; **7**: 79357-79364 [PMID: 27764817 DOI: 10.18632/oncotarget.12689]
- 76 Zhang Y, Kuang S, Shan Q, Rong D, Zhang Z, Yang H, Wu J, Chen J, He B, Deng Y, Roberts N, Shen J, Venkatesh SK, Wang J. Can IVIM help predict HCC recurrence after hepatectomy? *Eur Radiol* 2019; **29**: 5791-5803 [PMID: 30972544 DOI: 10.1007/s00330-019-06180-1]
- 77 Wei Y, Huang Z, Tang H, Deng L, Yuan Y, Li J, Wu D, Wei X, Song B. IVIM improves preoperative assessment of microvascular invasion in HCC. *Eur Radiol* 2019; **29**: 5403-5414 [PMID: 30877465 DOI: 10.1007/s00330-019-06088-w]
- 78 Zhao W, Liu W, Liu H, Yi X, Hou J, Pei Y, Liu H, Feng D, Liu L, Li W. Preoperative prediction of microvascular invasion of hepatocellular carcinoma with IVIM diffusion-weighted MR imaging and Gd-EOB-DTPA-enhanced MR imaging. *PLoS One* 2018; **13**: e0197488 [PMID: 29771954 DOI: 10.1371/journal.pone.0197488]
- 79 Li H, Zhang J, Zheng Z, Guo Y, Chen M, Xie C, Zhang Z, Mei Y, Feng Y, Xu Y. Preoperative histogram analysis of intravoxel incoherent motion (IVIM) for predicting microvascular invasion in patients with single hepatocellular carcinoma. *Eur J Radiol* 2018; **105**: 65-71 [PMID: 30017300 DOI: 10.1016/j.ejrad.2018.05.032]
- 80 Wagner M, Doblus S, Daire JL, Paradis V, Haddad N, Leitão H, Garteiser P, Vilgrain V, Sinkov R, Van Beers BE. Diffusion-weighted MR imaging for the regional characterization of liver tumors. *Radiology* 2012; **264**: 464-472 [PMID: 22692032 DOI: 10.1148/radiol.12111530]
- 81 Chiaradia M, Baranes L, Van Nhieu JT, Vignaud A, Laurent A, Decaens T, Charles-Nelson A, Brugnières P, Katsahian S, Djabbari M, Deux JF, Sobhani I, Karoui M, Rahmouni A, Luciani A. Intravoxel incoherent motion (IVIM) MR imaging of colorectal liver metastases: are we only looking at tumor necrosis? *J Magn Reson Imaging* 2014; **39**: 317-325 [PMID: 23723012 DOI: 10.1002/jmri.24172]
- 82 Yang L, Zhang XM, Tan BX, Liu M, Dong GL, Zhai ZH. Computed tomographic perfusion imaging for the therapeutic response of chemoembolization for hepatocellular carcinoma. *J Comput Assist Tomogr* 2012; **36**: 226-230 [PMID: 22446364 DOI: 10.1097/RCT.0b013e318245c23c]
- 83 Yang L, Zhang XM, Zhou XP, Tang W, Guan YS, Zhai ZH, Dong GL. Correlation between tumor perfusion and lipiodol deposition in hepatocellular carcinoma after transarterial chemoembolization. *J Vasc Interv Radiol* 2010; **21**: 1841-1846 [PMID: 20980165 DOI: 10.1016/j.jvir.2010.08.015]
- 84 Yang K, Zhang XM, Yang L, Xu H, Peng J. Advanced imaging techniques in the therapeutic response of transarterial chemoembolization for hepatocellular carcinoma. *World J Gastroenterol* 2016; **22**: 4835-4847 [PMID: 27239110 DOI: 10.3748/wjg.v22.i20.4835]
- 85 Pieper CC, Sprinkart AM, Meyer C, König R, Schild HH, Kukuk GM, Mürtz P. Evaluation of a Simplified Intravoxel Incoherent Motion (IVIM) Analysis of Diffusion-Weighted Imaging for Prediction of Tumor Size Changes and Imaging Response in Breast Cancer Liver Metastases Undergoing Radioembolization: A Retrospective Single Center Analysis. *Medicine (Baltimore)* 2016; **95**: e3275 [PMID: 27057887 DOI: 10.1097/MD.0000000000003275]
- 86 Wu L, Xu P, Rao S, Yang L, Chen C, Liu H, Fu C, Zeng M. ADC_{total} ratio and D ratio derived from intravoxel incoherent motion early after TACE are independent predictors for survival in hepatocellular carcinoma. *J Magn Reson Imaging* 2017; **46**: 820-830 [PMID: 28276105 DOI: 10.1002/jmri.25617]

- 87 **Shirot** N, Saito K, Sugimoto K, Takara K, Moriyasu F, Tokuyue K. Intravoxel incoherent motion MRI as a biomarker of sorafenib treatment for advanced hepatocellular carcinoma: a pilot study. *Cancer Imaging* 2016; **16**: 1 [PMID: 26822946 DOI: 10.1186/s40644-016-0059-3]
- 88 **Lee Y**, Lee SS, Cheong H, Lee CK, Kim N, Son WC, Hong SM. Intravoxel incoherent motion MRI for monitoring the therapeutic response of hepatocellular carcinoma to sorafenib treatment in mouse xenograft tumor models. *ActaRadiol* 2017; **58**: 1045-1053 [PMID: 28273738 DOI: 10.1177/0284185116683576]
- 89 **Park YS**, Lee CH, Kim JH, Kim IS, Kiefer B, Seo TS, Kim KA, Park CM. Using intravoxel incoherent motion (IVIM) MR imaging to predict lipiodol uptake in patients with hepatocellular carcinoma following transcatheter arterial chemoembolization: a preliminary result. *MagnReson Imaging* 2014; **32**: 638-646 [PMID: 24703575 DOI: 10.1016/j.mri.2014.03.003]
- 90 **Lin M**, Tian MM, Zhang WP, Xu L, Jin P. Predictive values of diffusion-weighted imaging and perfusion-weighted imaging in evaluating the efficacy of transcatheter arterial chemoembolization for hepatocellular carcinoma. *Onco Targets Ther* 2016; **9**: 7029-7037 [PMID: 27895495 DOI: 10.2147/OTT.S112555]
- 91 **Peng J**, Yang C, Zheng J, Wang R, Zhou Y, Wang W, Yang L, Zhang X, Miao N, Ren Y, Xu H, Min X. Intravoxel Incoherent Motion Diffusion Weighted Imaging for the Therapeutic Response of Transarterial Chemoembolization for Hepatocellular Carcinoma. *Journal of Cancer Therapy*. 2019; 591-60110.4236/jct.2019.107048]
- 92 **Wu LF**, Rao SX, Xu PJ, Yang L, Chen CZ, Liu H, Huang JF, Fu CX, Halim A, Zeng MS. Pre-TACE kurtosis of ADC_{total} derived from histogram analysis for diffusion-weighted imaging is the best independent predictor of prognosis in hepatocellular carcinoma. *EurRadiol* 2019; **29**: 213-223 [PMID: 29922932 DOI: 10.1007/s00330-018-5482-3]
- 93 **Server S**, Sabet S, Bilgin R, Inan N, Yuze Y, Tokat Y. Intravoxel Incoherent Motion Parameters for Assessing the Efficiency of Locoregional Bridging Treatments before Liver Transplantation. *Transplant Proc* 2019; **51**: 2391-2396 [PMID: 31474296 DOI: 10.1016/j.transproceed.2019.01.161]
- 94 **Lewin M**, Fartoux L, Vignaud A, Arrivé L, Menu Y, Rosmorduc O. The diffusion-weighted imaging perfusion fraction f is a potential marker of sorafenib treatment in advanced hepatocellular carcinoma: a pilot study. *EurRadiol* 2011; **21**: 281-290 [PMID: 20683597 DOI: 10.1007/s00330-010-1914-4]
- 95 **Yang SH**, Lin J, Lu F, Han ZH, Fu CX, Lv P, Liu H, Gao DM. Evaluation of antiangiogenic and antiproliferative effects of sorafenib by sequential histology and intravoxel incoherent motion diffusion-weighted imaging in an orthotopic hepatocellular carcinoma xenograft model. *J MagnReson Imaging* 2017; **45**: 270-280 [PMID: 27299302 DOI: 10.1002/jmri.25344]
- 96 **Joo I**, Lee JM, Han JK, Choi BI. Intravoxel incoherent motion diffusion-weighted MR imaging for monitoring the therapeutic efficacy of the vascular disrupting agent CKD-516 in rabbit VX2 liver tumors. *Radiology* 2014; **272**: 417-426 [PMID: 24697148 DOI: 10.1148/radiol.14131165]
- 97 **Ye W**, Li J, Guo C, Chen S, Liu YB, Liu Z, Wu H, Wang G, Liang C. Can intravoxel incoherent motion diffusion-weighted imaging characterize the cellular injury and microcirculation alteration in hepatic ischemia-reperfusion injury? An animal study. *J MagnReson Imaging* 2016; **43**: 1327-1336 [PMID: 26686869 DOI: 10.1002/jmri.25092]
- 98 **Ji Q**, Chu ZQ, Ren T, Xu SC, Zhang LJ, Shen W, Lu GM. Multiparametric functional magnetic resonance imaging for evaluation of hepatic warm ischemia-reperfusion injury in a rabbit model. *BMC Gastroenterol* 2017; **17**: 161 [PMID: 29246201 DOI: 10.1186/s12876-017-0720-8]
- 99 **Moon CM**, Shin SS, Lim NY, Kim SK, Kang YJ, Kim HO, Lee SJ, Beak BH, Kim YH, Jeong GW. Metabolic alterations in a rat model of hepatic ischaemia reperfusion injury: In vivo hyperpolarized ¹³C MRS and metabolic imaging. *Liver Int* 2018; **38**: 1117-1127 [PMID: 29345050 DOI: 10.1111/liv.13695]
- 100 **Abudurehman Y**, Wang J, Liu W. Comparison of Intravoxel Incoherent Motion Diffusion-Weighted Magnetic Resonance (MR) Imaging to T1 Mapping in Characterization of Hepatic Alveolar Echinococcosis. *Med SciMonit* 2017; **23**: 6019-6025 [PMID: 29259149 DOI: 10.12659/msm.903929]
- 101 **Ding L**, Xiao L, Lin X, Xiong C, Lin L, Chen S. Intravoxel Incoherent Motion (IVIM) Diffusion-Weighted Imaging (DWI) in Patients with Liver Dysfunction of Chronic Viral Hepatitis: Segmental Heterogeneity and Relationship with Child-Turcotte-Pugh Class at 3 Tesla. *Gastroenterol Res Pract* 2018; **2018**: 2983725 [PMID: 30647733 DOI: 10.1155/2018/2983725]
- 102 **Hong EK**, Joo I, Park J, Lee K. Assessment of hepatic sinusoidal obstruction syndrome with intravoxel incoherent motion diffusion-weighted imaging: An experimental study in a rat model. *J MagnReson Imaging* 2020; **51**: 81-89 [PMID: 31094055 DOI: 10.1002/jmri.26790]



Published by **Baishideng Publishing Group Inc**
7041 Koll Center Parkway, Suite 160, Pleasanton, CA 94566, USA

Telephone: +1-925-3991568

E-mail: bpgoffice@wjgnet.com

Help Desk: <https://www.f6publishing.com/helpdesk>

<https://www.wjgnet.com>

